On three-dimensional long interfacial wave propagation near the critical depth level

Yongze Chen
Center for Coastal Studies, Scripps Institution of Oceanography, La Jolla, CA 92093

Philip L.-F. Liu
School of Civil and Environmental Engineering, Cornell University, Ithaca, NY 14853

Short title:

Abstract.

In this paper, the propagation of interfacial waves near the critical depth level in a two-layered fluid system is investigated. We first derive an evolution equation for weakly nonlinear and dispersive interfacial waves propagating predominantly in the longitudinal direction of a slowly rotating channel with gradually varying topography and sidewalls. The new evolution equation includes both quadratic and cubic nonlinearities. For interfacial waves propagating in certain type of non-rotating channels with varying topography, we find two families of periodic solutions, expressed in terms of the snoidal function, to the variable-coefficient equation. As the limiting cases of these periodic-wave solutions, a family of solitary-wave solutions and an isolated shock-like wave solution are also obtained. In a uniform rotating channel, our small-time asymptotic analysis and numerical study show that depending on the relative importance of the cubic nonlinearity to quadratic nonlinearity, the wavefront of a Kelvin solitary wave will curve either forwards or backwards, trailed by a small train of Poincaré waves. When these two nonlinearities almost balance each other, the wavefront becomes almost straight-crested across the channel, and the trailing Poincaré waves diminish.

1. Introduction

Nonlinear and dispersive internal wave trains have been observed and measured in marine straits (e.g. Gargett 1976; Alpers & Salusti 1983; La Violette & Arnone 1988) and in long, narrow thermally stratified lakes (e.g. Thorpe, Hall & Crofts 1972; Hunkins & Fliegel 1973; Farmer 1978). Many attempts have been made to extend the applicability of the original Kadomtsev–Petviashvili (KP) equation (Kadomtsev & Petviashvili 1970) to accommodate important factors affecting these observed internal wave propagations, such as rotation, variations of topography and sidewalls, and a background current field. Most recently, Chen & Liu (1995) presented the derivation of the unified KP (uKP) equation for weakly nonlinear and dispersive interfacial waves of two-layer fluids propagating predominantly in the longitudinal direction of a slowly rotating channel with gradually varying topography and sidewalls, and a weak steady background current field. Their result was a generalization of all previous work within the context of surface and interfacial waves.

The uKP equation was derived under the assumption that the effects of nonlinearity, dispersion, rotation, transverse modulation and variations of topography and sidewalls are weak but equally important. In the equation, the nonlinear term is quadratic and its coefficient is proportional to $D_{-2} = \rho^-/(h^-)^2 - \rho^+/(h^+)^2$, where $\rho^\pm$ and $h^\pm$ are the dimensionless densities and leading-order depths in the upper and lower layers, respectively. This implicitly limits the range of the variation of topography because D_{-2} must remain same sign and be an order one quantity to ensure that the nonlinearity indeed is as important as the dispersion and other effects. If the bottom changes to certain extent that D_{-2} changes sign, the uKP equation is no longer applicable because near the critical depth level defined as $h^+/h^- = (\rho^+/\rho^-)^{1/2}$(i.e. $D_{-2} = 0$), the coefficient of the nonlinear term is so small that the balance between the nonlinearity and dispersion (and other effects) becomes impossible under the Boussinesq assumption, i.e. $O(a_0/h_0) = O(h_0^2/l_0^2) \ll 1$, where a_0, h_0 and l_0 are the typical wave amplitude, depth

and wavelength, respectively.

In the study of the change of polarity of two-dimensional solitary waves as they pass through the critical depth level, Helfrich, Melville & Miles (1984) showed that near the critical depth level, nonlinearity and dispersion can be of the same order magnitude in the parametric regime where $O(a_0/h_0) = O(h_0/l_0) \ll 1$. In this situation, the cubic nonlinearity becomes comparable to or dominates the quadratic nonlinearity and must be taken into account.

The inclusion of the cubic nonlinearity can have a significant influence on wave motion. For transcritical two-layer flow over a two-dimensional topography or past a constriction in a stationary channel, Melville and his associates found that the inclusion of the cubic nonlinearity changes the character of the upstream disturbance, giving an upstream advancing monotonic non-dissipative bore, rather than a trains of Boussinesq solitary waves (Melville & Helfrich 1987; Tomasson & Melville 1991).

Although recently there have been several studies on Kelvin solitary wave propagation in a rotating channel (Katsis & Akylas 1987; Melville, Tomasson & Renouard 1989; Grimshaw & Tang 1990; Chen & Liu 1996*b*), Kelvin solitary wave propagation near the critical depth level has not been studied yet. We expect that the inclusion of the cubic nonlinearity may give rise to some new wave propagation phenomena, especially when the Kelvin solitary wave propagates over a varying topography such that the coefficient of the quadratic nonlinear term changes its sign.

In this paper, we consider the formulation and analytical solutions of the evolution equation that governing three-dimensional interfacial wave propagation near the critical depth level in the most possible general setting. Then, we apply the equation to study Kelvin solitary wave propagation near the critical depth level in a rotating uniform channel to reveal new wave phenomena caused by the cubic nonlinearity.

In the next section, assuming that the effects of nonlinearity, dispersion, rotation, transverse modulation and variations of topography and sidewalls are weak but

equally important, we derive an interfacial displacement evolution equation for waves propagating near the critical depth level. In section 3, we study the integrability of the evolution equation and seek analytical solutions to describe wave propagations in certain type of curved channels with varying topography. In section 4, we carry out the small-time asymptotic analysis and numerical study of the evolution equation for Kelvin solitary wave propagation in a rotating uniform channel to examine the physical features brought by the cubic nonlinearity. Concluding remarks are given in section 5.

2. Derivation of the evolution equation

We consider interfacial waves propagating along the interface of two fluid layers confined in a rotating wide channel with varying topography and sidewalls. Cartesian coordinates are employed with the $\tilde{x}$- and $\tilde{y}$-axis in the longitudinal and transverse directions of the channel, respectively, and the $\tilde{z}$-axis pointing vertically upwards. The interface is denoted by $\tilde{z} = \tilde{\eta}(\tilde{x}, \tilde{y}, \tilde{t})$ with $\tilde{z} = 0$ being the undisturbed interface. The rotation rate about the vertical axis is $f/2$. The densities of the upper and lower layers are $\tilde{\rho}^+$ and $\tilde{\rho}^-$ ($\tilde{\rho}^- > \tilde{\rho}^+$), respectively (hereafter superscripts $+$ and $-$ are used to identify quantities in the upper and lower layers, respectively). The upper and lower layers are bounded by $\tilde{z} = \tilde{H}^+$ (the rigid-lid assumption is adopted to approximate the free surface) and $\tilde{z} = \tilde{H}^-(\tilde{x}, \tilde{y})$, respectively. The vertical sidewalls are represented by $\tilde{y} = \tilde{y}_l(\tilde{x})$ and $\tilde{y} = \tilde{y}_r(\tilde{x})$ with $\tilde{y}_l > \tilde{y}_r$.

The fluids in both layers are assumed to be inviscid and incompressible. The dimensionless governing equations and boundary conditions for flows in the upper and lower layers are

$$\frac{\partial u^\pm}{\partial x} + \frac{\partial v^\pm}{\partial y} + \frac{\partial w^\pm}{\partial z} = 0, \tag{2.1a}$$

$$\frac{\partial u^\pm}{\partial t} + \epsilon \left(u^\pm \frac{\partial u^\pm}{\partial x} + v^\pm \frac{\partial u^\pm}{\partial y} + w^\pm \frac{\partial u^\pm}{\partial z} \right) - \gamma v^\pm = -\frac{\partial p^\pm}{\partial x}, \tag{2.1b}$$

$$\frac{\partial v^{\pm}}{\partial t}+\epsilon\left(u^{\pm}\frac{\partial v^{\pm}}{\partial x}+v^{\pm}\frac{\partial v^{\pm}}{\partial y}+w^{\pm}\frac{\partial v^{\pm}}{\partial z}\right)+\gamma u^{\pm}=-\frac{\partial p^{\pm}}{\partial y}, \tag{2.1c}$$

$$\mu^2\left[\frac{\partial w^{\pm}}{\partial t}+\epsilon\left(u^{\pm}\frac{\partial w^{\pm}}{\partial x}+v^{\pm}\frac{\partial w^{\pm}}{\partial y}+w^{\pm}\frac{\partial w^{\pm}}{\partial z}\right)\right]=-\frac{\partial p^{\pm}}{\partial z}, \tag{2.1d}$$

$$w^{\pm}=\frac{\partial \eta}{\partial t}+\epsilon\left(u^{\pm}\frac{\partial \eta}{\partial x}+v^{\pm}\frac{\partial \eta}{\partial y}\right) \quad \text{on} \quad z=\epsilon\eta, \tag{2.1e}$$

$$\rho^{+}p^{+}-\rho^{-}p^{-}+\eta=0 \quad \text{on} \quad z=\epsilon\eta, \tag{2.1f}$$

$$w^{+}=0 \quad \text{on} \quad z=H^{+}, \tag{2.1g}$$

$$w^{-}=-u^{-}\frac{\partial H^{-}}{\partial x}-v^{-}\frac{\partial H^{-}}{\partial y} \quad \text{on} \quad z=-H^{-}(x,y), \tag{2.1h}$$

$$v^{\pm}=u^{\pm}\frac{\mathrm{d}y}{\mathrm{d}x} \quad \text{on} \quad y=y_r(x), y_l(x), \tag{2.1i}$$

where superscripts $\pm$ are vertically ordered; $u^{\pm}, v^{\pm}$ and $w^{\pm}$ are the dimensionless velocity components in the x-, y- and z-direction, respectively, and $p^{\pm}$ is the dimensionless hydrodynamic pressure. The dimensionless variables are related to their dimensional counterparts (denoted by tildes) by:

$$\left.\begin{gathered}(\tilde{x},\tilde{y})=l_0(x,y), \quad \tilde{z}=h_0 z, \quad \tilde{t}=\frac{l_0}{c_0}t, \quad \tilde{H}^{\pm}=h_0H^{\pm}, \quad \tilde{y}_r=l_0y_r,\\ \tilde{y}_l=l_0y_l, \quad \tilde{\eta}=a_0\eta, \quad (\tilde{u}^{\pm},\tilde{v}^{\pm})=\frac{a_0c_0}{h_0}(u^{\pm},v^{\pm}), \quad \tilde{w}^{\pm}=\frac{a_0c_0}{l_0}w^{\pm},\\ \tilde{\rho}^{\pm}=\rho_0\rho^{\pm}, \quad c_0^2=(\rho^{-}-\rho^{+})gh_0, \quad \tilde{p}^{\pm}=\frac{a_0}{h_0}c_0^2\rho_0\rho^{\pm}p^{\pm},\end{gathered}\right\} \tag{2.2}$$

where l_0 and h_0 are the characteristic wavelength and depth, respectively; a_0 and c_0 are the characteristic amplitude and phase speed of linear long waves, respectively; g is the gravitational acceleration and ρ_0 is the characteristic density. The parameters ϵ, μ^2 and γ appearing in (2.1) are defined as

$$\epsilon=a_0/h_0, \qquad \mu^2=(h_0/l_0)^2, \qquad \gamma=l_0f/c_0, \tag{2.3}$$

which measure nonlinearity, dispersion and rotation, respectively.

We shall derive the evolution equation for weakly nonlinear and dispersive interfacial waves propagating near the critical depth level and travelling predominantly in the

longitudinal direction of a slowly rotating channel with gradually varying topography and sidewalls. More specifically, we assume that

$$D_{-2} = \rho^-/(h^-)^2 - \rho^+/(h^+)^2 = O(\epsilon), \quad \epsilon = \alpha\mu, \quad \gamma = \beta\mu, \quad \text{with } \mu \ll 1, \tag{2.4}$$

where α and β are two order one constants, and the bottom and the sidewalls can be expressed as

$$H^- = h^-(\mu^2 x) + \mu^2 B(\mu^2 x, \mu y), \tag{2.5a}$$

$$y_r = \frac{1}{\mu} Y_R(\mu^2 x), \qquad y_l = \frac{1}{\mu} Y_L(\mu^2 x). \tag{2.5b}$$

We use μ as the basic perturbation parameter in the following derivation.

To derive a single evolution equation for the interfacial displacement, we introduce the following transformation:

$$\xi = \int_0^x C^{-1}(\mu^2 x)\mathrm{d}x - t, \qquad X = \mu^2 x, \qquad Y = \mu y, \qquad Z = z, \tag{2.6a}$$

where C is given by

$$C(X) = \left(\rho^+/h^+ + \rho^-/h^-\right)^{-1/2}, \tag{2.6b}$$

and $h^+ \equiv H^+ \equiv$ constant is used for convenience. Note that C is the leading order of the local linear-long-wave speed and $\xi = O(1)$ is the characteristic coordinate moving at the speed of C to the right.

In the moving coordinates (ξ, X, Y, Z), governing equations and boundary conditions (2.1) can be rewritten as

$$\frac{1}{C}\frac{\partial u^\pm}{\partial \xi} + \mu^2 \frac{\partial u^\pm}{\partial X} + \mu \frac{\partial v^\pm}{\partial Y} + \frac{\partial w^\pm}{\partial Z} = 0, \tag{2.7a}$$

$$\begin{aligned} \frac{\partial u^\pm}{\partial \xi} &- \alpha\mu \left[u^\pm \left(\frac{1}{C}\frac{\partial u^\pm}{\partial \xi} + \mu^2 \frac{\partial u^\pm}{\partial X} \right) + \mu v^\pm \frac{\partial u^\pm}{\partial Y} + w^\pm \frac{\partial u^\pm}{\partial Z} \right] + \beta\mu v^\pm \\ &= \frac{1}{C}\frac{\partial p^\pm}{\partial \xi} + \mu^2 \frac{\partial p^\pm}{\partial X}, \end{aligned} \tag{2.7b}$$

$$\frac{\partial v^\pm}{\partial \xi} - \alpha\mu \left[u^\pm \left(\frac{1}{C}\frac{\partial v^\pm}{\partial \xi} + \mu^2 \frac{\partial v^\pm}{\partial X} \right) + \mu v^\pm \frac{\partial v^\pm}{\partial Y} + w^\pm \frac{\partial v^\pm}{\partial Z} \right] - \beta\mu u^\pm = \mu \frac{\partial p^\pm}{\partial Y}, \tag{2.7c}$$

$$\mu^2\left\{\frac{\partial w^{\pm}}{\partial \xi}-\alpha\mu\left[u^{\pm}\left(\frac{1}{C}\frac{\partial w^{\pm}}{\partial \xi}+\mu^2\frac{\partial w^{\pm}}{\partial X}\right)+\mu v^{\pm}\frac{\partial w^{\pm}}{\partial Y}+w^{\pm}\frac{\partial w^{\pm}}{\partial Z}\right]\right\}=\frac{\partial p^{\pm}}{\partial Z}, \tag{2.7d}$$

$$w^{\pm}=-\frac{\partial \eta}{\partial \xi}+\alpha\mu\left[u^{\pm}\left(\frac{1}{C}\frac{\partial \eta}{\partial \xi}+\mu^2\frac{\partial \eta}{\partial X}\right)+\mu v^{\pm}\frac{\partial \eta}{\partial Y}\right] \quad \text{on} \quad Z=\epsilon\eta, \tag{2.7e}$$

$$\rho^{+}p^{+}-\rho^{-}p^{-}+\eta=0 \quad \text{on} \quad Z=\epsilon\eta, \tag{2.7f}$$

$$w^{+}=0 \quad \text{on} \quad Z=h^{+}, \tag{2.7g}$$

$$w^{-}=-\mu^2u^{-}\left(\frac{\mathrm{d}h^{-}}{\mathrm{d}X}+\mu^2\frac{\partial B}{\partial X}\right)-\mu^3v^{-}\frac{\partial B}{\partial Y} \quad \text{on} \quad Z=-h^{-}-\mu^2B, \tag{2.7h}$$

$$v^{\pm}=\mu u^{\pm}\frac{\mathrm{d}Y}{\mathrm{d}X} \quad \text{on} \quad Y=Y_R(X),Y_L(X), \tag{2.7i}$$

where (2.5a) and (2.5b) have been used.

A solution to the governing equations and boundary conditions (2.7) is sought in the following series forms:

$$G=G_0(\xi,X,Y,Z)+\mu G_1(\xi,X,Y,Z)+\mu^2G_2(\xi,X,Y,Z)+O(\mu^3), \tag{2.8a}$$

$$v^{\pm}=\mu v_1^{\pm}(\xi,X,Y,Z)+\mu^2v_2^{\pm}(\xi,X,Y,Z)+O(\mu^3), \tag{2.8b}$$

$$\eta=\eta_0(\xi,X,Y)+\mu\eta_1(\xi,X,Y)+\mu^2\eta_2(\xi,X,Y)+O(\mu^3), \tag{2.8c}$$

where $G=\{u^{\pm},w^{\pm},p^{\pm}\}$. Substituting (2.8) into (2.7) and expanding the interfacial boundary conditions (2.7e) and (2.7f) at $Z=0$ and the bottom boundary condition (2.7h) at $Z=-h^{-}$, we obtain a sequence of initial-boundary-value problems by collecting coefficients of μ^n. Carrying out the perturbation analysis to the second order ($n=2$), we find out that the compatibility condition of the second-order problem requires η_0 and η_1 to satisfy the following evolution equation (for details, see Chen 1995):

$$\begin{aligned}&C^{1/2}\frac{\partial}{\partial X}\left(C^{1/2}\frac{\partial \eta_0}{\partial \xi}\right)+\frac{3\alpha C^2}{4\mu}D_{-2}\frac{\partial^2\eta_0^2}{\partial \xi^2}-\alpha^2C^2D_{-3}\frac{\partial^2\eta_0^3}{\partial \xi^2}+\frac{D_1}{6}\frac{\partial^4\eta_0}{\partial \xi^4}\\&+\frac{C^2}{2}\frac{\partial^2\eta_0}{\partial Y^2}-\frac{\beta^2}{2}\eta_0+\frac{\rho^{-}BC^2}{2(h^{-})^2}\frac{\partial^2\eta_0}{\partial \xi^2}+\frac{3\alpha C^2}{2}D_{-2}\frac{\partial^2\eta_0\eta_1}{\partial \xi^2}=0,\end{aligned} \tag{2.9}$$

where D_1, D_{-2} and D_{-3} are defined as

$$D_n(X) = \rho^-(h^-)^n + (-1)^{n-1}\rho^+(h^+)^n \quad (n = 1, -2, -3). \tag{2.10}$$

Because $D_{-2} = \rho^-/(h^-)^2 - \rho^+/(h^+)^2 = O(\epsilon)$, the last term involving η_1 in (2.9) can be dropped and we obtain the evolution equation, including both quadratic and cubic nonlinearity, for interfacial waves propagating near the critical depth level:

$$\begin{aligned} C^{1/2}\frac{\partial}{\partial X}\left(C^{1/2}\frac{\partial \eta_0}{\partial \xi}\right) &+ \frac{3\epsilon}{4\mu^2}C^2 D_{-2}\frac{\partial^2 \eta_0^2}{\partial \xi^2} - \frac{\epsilon^2}{\mu^2}C^2 D_{-3}\frac{\partial^2 \eta_0^3}{\partial \xi^2} + \frac{D_1}{6}\frac{\partial^4 \eta_0}{\partial \xi^4} \\ &+ \frac{C^2}{2}\frac{\partial^2 \eta_0}{\partial Y^2} - \frac{\gamma^2}{2\mu^2}\eta_0 + \frac{\rho^- B C^2}{2(h^-)^2}\frac{\partial^2 \eta_0}{\partial \xi^2} = 0. \end{aligned} \tag{2.11}$$

The leading order of the impermeable boundary conditions along the sidewalls, (2.7i), provides the sidewall boundary conditions for η_0:

$$\frac{\partial \eta_0}{\partial Y} + \frac{\gamma}{\mu C}\eta_0 = \frac{1}{C}\frac{\mathrm{d}Y}{\mathrm{d}X}\frac{\partial \eta_0}{\partial \xi} \quad \text{on } Y = Y_R(X), Y_L(X). \tag{2.12}$$

Note that if $O(\epsilon) = O(\mu^2)$ and $D_{-2} = O(1)$, the cubic nonlinear term in (2.11) becomes higher-order and can be neglected; the resulting equation recovers the uKP equation derived by Chen & Liu (1995) through the following changes:

$$(X, Y, B) \mapsto \left(\frac{\mu^2}{\epsilon}X, \frac{\mu}{\epsilon^{1/2}}Y, \frac{\epsilon}{\mu^2}B\right). \tag{2.13}$$

The boundary conditions on the sidewalls for the uKP equation are also recovered from (2.12) through the same changes. Besides the cubic nonlinear term, the physical meaning of each of the remaining terms in (2.11) is the same as that of the corresponding term in the uKP equation (Chen & Liu 1995).

In the absence of rotation, (2.11) can be further reduced to the existing evolution equations for interfacial wave propagation near the critical depth level. For example, if the bottom is flat, (2.11) becomes:

$$\frac{\partial^2 \eta_0}{\partial X \partial \xi} + \frac{3\epsilon}{4\mu^2}C D_{-2}\frac{\partial^2 \eta_0^2}{\partial \xi^2} - \frac{\epsilon^2}{\mu^2}C D_{-3}\frac{\partial^2 \eta_0^3}{\partial \xi^2} + \frac{D_1}{6C}\frac{\partial^4 \eta_0}{\partial \xi^4} + \frac{C}{2}\frac{\partial^2 \eta_0}{\partial Y^2} = 0, \tag{2.14}$$

which agrees with the modified KP equation given by Tsuji & Oikawa (1993), who numerically solved the equation to study the interaction of two solitary waves propagating in close directions. On the other hand, if the wave field is independent of Y (the sidewalls should be straight and parallel), (2.11) reduces to

$$C^{1/2}\frac{\partial}{\partial X}\left(C^{1/2}\eta_0\right)+\frac{3\epsilon}{4\mu^2}C^2D_{-2}\frac{\partial\eta_0^2}{\partial\xi}-\frac{\epsilon^2}{\mu^2}C^2D_{-3}\frac{\partial\eta_0^3}{\partial\xi}+\frac{D_1}{6}\frac{\partial^3\eta_0}{\partial\xi^3}+\frac{\rho^-BC^2}{2(h^-)^2}\frac{\partial\eta_0}{\partial\xi}=0. \quad (2.15)$$

When $B=0$, (2.15) is equivalent to the evolution equation derived by Helfrich *et al.* (1984). When h^- is constant, (2.15) is identical to the evolution equation derived by Chen & Liu (1996*a*) to study the effect of a random topography on two-dimensional interfacial wave propagation.

Assuming that the solution of (2.11) with boundary conditions (2.12), η_0, is locally confined, we find out that

$$\mathcal{I}=(C/W)^{1/2}\int_{Y_R}^{Y_L}\int_{-\infty}^{+\infty}\eta_0 \mathrm{d}\xi \mathrm{d}Y, \quad W(X)=Y_L(X)-Y_R(X) \quad (2.16)$$

is the first-order invariant when the rotation is absent (i.e. $\gamma=0$) and

$$\mathcal{J}=C\int_{Y_R}^{Y_L}\int_{-\infty}^{+\infty}\eta_0^2 \mathrm{d}\xi \mathrm{d}Y \quad (2.17)$$

is the second-order invariant regardless whether the rotation is present. The locally confined solution also has to satisfy the same constraint imposed on the uKP equation (Chen & Liu 1995):

$$\int_{-\infty}^{+\infty}\eta_0 \mathrm{d}\xi = F(X)\exp(-\beta Y/C). \quad (2.18)$$

Thus, again, the minimal requirement for a solution of (2.11) with (2.12) to be locally confined is that its initial condition satisfies (2.18) (with $\beta=\gamma/\mu$) at $X=0$.

3. Analytic solutions

Equation (2.11) is a nonlinear evolution equation with variable coefficients. In general, no procedure is available to obtain analytic solutions of the corresponding

Cauchy problem, let alone initial-boundary-value problems. In this section, we focus on initial-value problems first.

A powerful tool to investigate the complete integrability of a nonlinear evolution equation is the Painlevé PDE test (Ablowitz & Clarkson 1991). It provides a useful criterion for whether a given partial differential equation is completely integrable. We now carry out the Painlevé analysis to find out under what conditions (2.11) passes the test, as we did for the uKP equation in Chen & Liu (1995).

To simplify the algebraic manipulation, we introduce the following transformation:

$$\eta_0 = \frac{\mu}{\epsilon C}\left(\frac{D_1}{3D_{-3}}\right)^{1/2}\zeta, \quad \tau = \int_0^X \frac{D_1}{6C}\mathrm{d}X, \tag{3.1}$$

which transforms (2.11) into

$$\frac{\partial^2\zeta}{\partial\tau\partial\xi} + e(\tau)\frac{\partial^2\zeta^2}{\partial\xi^2} - 2\frac{\partial^2\zeta^3}{\partial\xi^2} + \frac{\partial^4\zeta}{\partial\xi^4} + a(\tau)\frac{\partial^2\zeta}{\partial Y^2} + b(\tau,Y)\frac{\partial^2\zeta}{\partial\xi^2} + c(\tau)\frac{\partial\zeta}{\partial\xi} - d(\tau)\zeta = 0, \tag{3.2}$$

where

$$a = 3C^2/D_1, \quad b = \frac{3\rho^- BC^2}{D_1(h^-)^2}, \tag{3.3a}$$

$$c = \frac{3\rho^- C}{D_1(h^-)^4}\left[\frac{(h^-)^4}{D_1} + \frac{3}{D_{-3}} - \frac{C^2(h^-)^2}{2}\right]\frac{\mathrm{d}h^-}{\mathrm{d}X}, \tag{3.3b}$$

$$d = \frac{3\gamma^2}{\mu^2 D_1}, \quad e = \frac{3CD_{-2}}{2\mu}\left(\frac{3}{D_1 D_{-3}}\right)^{1/2}. \tag{3.3c}$$

We seek solutions of (3.2) in the form

$$\zeta(\tau,\xi,Y) = \varphi^p\sum_{j=0}^{\infty} u_j(\tau,Y)\varphi^j, \qquad \varphi(\tau,\xi,Y) = \xi + \psi(\tau,Y), \tag{3.4}$$

where p is an integer, and $\psi(\tau,Y)$ and $u_j(\tau,Y)(j=0,1,2,\ldots)$ are analytic functions of τ and Y in the neighborhood of a non-characteristic movable singularity manifold defined by $\varphi = 0$. Upon substitution of (3.4) into (3.2), the leading-order analysis requires that $p = -1$ and $u_0^2 = 1$. Equating the like powers of φ yields the general recursion relation:

$$(j+1)(j-3)(j-4)^2 u_j + W_j = 0, \tag{3.5a}$$

where

$$
\begin{aligned}
W_j \;=\; & a\frac{\partial^2 u_{j-4}}{\partial Y^2} - d u_{j-4} - 2(j-3)(j-4)\left[\sum_{k=1}^{j-1}\sum_{m=0}^{k} u_m u_{j-k} u_{k-m} + u_0 \sum_{m=1}^{j-1} u_m u_{j-m}\right] \\
& + e(j-3)(j-4)\sum_{k=0}^{j-1} u_k u_{j-1-k} + (j-3)(j-4)u_{j-2}\left[\frac{\partial \psi}{\partial \tau} + a\left(\frac{\partial \psi}{\partial Y}\right)^2 + b\right] \\
& + (j-4)\left[u_{j-3}\left(c + a\frac{\partial^2 \psi}{\partial Y^2}\right) + \frac{\partial u_{j-3}}{\partial \tau} + 2a\frac{\partial \psi}{\partial Y}\frac{\partial u_{j-3}}{\partial Y}\right] \qquad (3.5b)
\end{aligned}
$$

for $j \geq 1$ (define $u_j = 0$ for $j < 0$).

Since $j = 4$ is a double root of the indicial polynomial determining the resonances (occurring at some j where u_j is arbitrary), (3.2) cannot pass the Painlevé test. Note that the appearance of the double root is due to the existence of the cubic nonlinear term in (3.2); even for the simplest case when the rotation is absent and the bottom is flat, the equation still cannot pass the Painlevé test. Since there is no way to let (3.2) pass the Painlevé test by imposing restrictions on the variable coefficients a, b, c, d and e (if there were, the evolution equation could be reduced to a completely integrable equation in canonical form via an elementary transformation), the search for analytical solutions of (3.2) or (2.11) becomes very challenging. In what follows, we shall give some analytical solutions to (2.11) for certain type of varying topography and sidewalls in the absence of rotation.

Under the assumption that

$$
\beta = 0, \quad h^- = \text{const}, \quad \frac{\rho^- BC}{2(h^-)^2} = F_1(X)Y + F_0(X), \qquad (3.6)
$$

where F_0 and F_1 are arbitrary functions of X, (2.11) becomes:

$$
\begin{aligned}
\frac{\partial^2 \eta_0}{\partial X \partial \xi} \;+\; & \frac{3\alpha}{4\mu} C D_{-2} \frac{\partial^2 \eta_0^2}{\partial \xi^2} - \alpha^2 C D_{-3} \frac{\partial^2 \eta_0^3}{\partial \xi^2} + \frac{D_1}{6C}\frac{\partial^4 \eta_0}{\partial \xi^4} \\
+ \; & \frac{C}{2}\frac{\partial^2 \eta_0}{\partial Y^2} + [F_1(X)Y + F_0(X)]\frac{\partial^2 \eta_0}{\partial \xi^2} = 0, \qquad (3.7)
\end{aligned}
$$

which is still a nonlinear evolution equation with variable coefficients. Assumption (3.6) implies that there is no rotation and the variation of topography is weak and behaves

like a linear function in the transverse direction. Note that this assumption actually is the complete integrability conditions for the uKP equation (Chen & Liu 1995).

We find that the following transformation:

$$\eta_0 = \frac{1}{\alpha C}\sqrt{D_1/D_{-3}}\,\zeta, \tag{3.8a}$$

$$\bar{T} = \sqrt{6}D_1 X/C, \tag{3.8b}$$

$$\bar{X} = \sqrt{6}\left\{\xi - Y\int_0^X F_1(q)\mathrm{d}q - \int_0^X \left[F_0(q) + \frac{C}{2}\left(\int_0^q F_1(s)\mathrm{d}s\right)^2\right]\mathrm{d}q\right\}, \tag{3.8c}$$

$$\bar{Y} = 6\sqrt{D_1}\left[Y/C + \int_0^X\int_0^q F_1(s)\mathrm{d}s\mathrm{d}q\right], \tag{3.8d}$$

transforms equation (3.7) and boundary conditions (2.12) with $\gamma = 0$ (i.e. $\beta = 0$) into

$$\frac{\partial}{\partial\bar{X}}\left(\frac{\partial\zeta}{\partial\bar{T}} + 6r\zeta\frac{\partial\zeta}{\partial\bar{X}} - 3\zeta^2\frac{\partial\zeta}{\partial\bar{X}} + \frac{\partial^3\zeta}{\partial\bar{X}^3}\right) + 3\frac{\partial^2\zeta}{\partial\bar{Y}^2} = 0, \tag{3.9}$$

with

$$r = \frac{CD_{-2}}{4\mu(D_1D_{-3})^{1/2}}, \tag{3.10}$$

and

$$\frac{\partial\zeta}{\partial\bar{Y}} = (6D_1)^{-1/2}\left[\frac{\mathrm{d}Y_R}{\mathrm{d}X} + C\int_0^X F_1(q)\mathrm{d}q\right]\frac{\partial\zeta}{\partial\bar{X}} \quad \text{on} \quad \bar{Y} = \bar{Y}_R(\bar{T}), \tag{3.11a}$$

$$\frac{\partial\zeta}{\partial\bar{Y}} = (6D_1)^{-1/2}\left[\frac{\mathrm{d}Y_L}{\mathrm{d}X} + C\int_0^X F_1(q)\mathrm{d}q\right]\frac{\partial\zeta}{\partial\bar{X}} \quad \text{on} \quad \bar{Y} = \bar{Y}_L(\bar{T}), \tag{3.11b}$$

respectively, where

$$\bar{Y}_R(\bar{T}) = 6\sqrt{D_1}\left[Y_R/C + \int_0^X\int_0^q F_1(s)\mathrm{d}s\mathrm{d}q\right], \tag{3.12a}$$

$$\bar{Y}_L(\bar{T}) = 6\sqrt{D_1}\left[Y_L/C + \int_0^X\int_0^q F_1(s)\mathrm{d}s\mathrm{d}q\right]. \tag{3.12b}$$

As shown in (3.10), the parameter r signifies the relative importance of the quadratic and cubic nonlinearities. Note that with a rescaling, (3.8) is equivalent to the transformation used to transform the uKP equation (under assumption (3.6)) into the KP equation in canonical form (Chen & Liu 1995).

Equation (3.9) is a constant-coefficient modified KP equation. Although the KP equation and the modified KdV equation are both completely integrable, the modified KP equation (3.9) is not (note that (3.9) is a special case of (3.2)). Nevertheless, since (3.9) is a constant-coefficient wave equation, it may admit travelling-wave solutions. We now seek for all bounded travelling-wave solutions of (3.9). Substituting $\zeta(\phi) = \zeta(\bar{X} + l\bar{Y} - \omega\bar{T})$ (l and ω are constants) into (3.9) and integrating the resulting equation twice, we obtain

$$\zeta'' = \zeta^3 - 3r\zeta^2 + (\omega - 3l^2)\zeta + A\phi + B, \tag{3.13}$$

where $' = \mathrm{d}/\mathrm{d}\phi$, A and B are two constants of integration. For bounded solutions, A must be zero. Therefore, (3.13) can be recast into

$$\chi' = \vartheta, \qquad \vartheta' = \chi^3 - p\chi + q, \tag{3.14a}$$

where

$$\zeta = \chi + r, \quad p = 3r^2 + 3l^2 - \omega, \quad q = B + (\omega - 3l^2)r - 2r^3. \tag{3.14b}$$

Carrying out the analysis in the phase plane (χ, ϑ) (for details, see appendix), we find two families of periodic solutions (corresponding to close orbits in the (χ, ϑ)-plane) for (3.9), which are given as follows.

The first family of periodic solutions to (3.9) is given by

$$\begin{aligned} \zeta = r \;&-\; H[m(3-2n) - n(2-n)][4n(m-n)]^{-1} \\ &+\; H(1/n - 1)\left[1 - n\mathrm{sn}^2(\Phi, m)\right]^{-1}, \end{aligned} \tag{3.15a}$$

with

$$\Phi = K\sec\theta_0\bar{\phi} + \Phi_0 = K\sec\theta_0\left(\cos\theta_0\bar{X} + \sin\theta_0\bar{Y} - V\bar{T}\right) + \Phi_0, \tag{3.15b}$$

$$K = H\sqrt{(1-n)[8n(m-n)]^{-1}}, \tag{3.15c}$$

$$\begin{aligned} V \;=\; &\cos\theta_0\left\{3r^2 + 3\tan^2\theta_0 - H^2[m^2(3 - 4n + 4n^2)\right. \\ &\left. - 2mn(2 - n + 2n^2) + n^2(4 - 4n + 3n^2)][4n(m-n)]^{-2}\right\}, \end{aligned} \tag{3.15d}$$

where H is the wave height, m and n $(0 < n < m < 1)$ are two parameters, θ_0 is the angle of incidence, K is the $\bar{X}$-component wavenumber, V is the phase speed and Φ_0 is a phase constant. The wavelength of the periodic wave (3.15), Λ, is given by

$$\Lambda = 2\mathrm{K}(m)\cos\theta_0/K, \tag{3.16}$$

where

$$\mathrm{K}(m) = \int_0^{\pi/2} \frac{\mathrm{d}t}{[1 - m\sin^2 t]^{1/2}} \tag{3.17}$$

is the complete elliptic integral of the first kind.

Assuming that the mean interface is located at $z = 0$, i.e. the net area covered by the interface within a wavelength is zero:

$$\int_0^{\Lambda} \zeta\left(\frac{2\mathrm{K}(m)}{\Lambda}\bar{\phi}\right)\mathrm{d}\bar{\phi} = \frac{\Lambda}{2\mathrm{K}(m)}\int_0^{2\mathrm{K}(m)} \zeta(\Phi)\mathrm{d}\Phi = 0, \tag{3.18}$$

we obtain

$$(1 - 1/n)\Pi(n,m)/\mathrm{K}(m) = r/H - [m(3-2n) - n(2-n)]\left[4n(m-n)\right]^{-1}, \tag{3.19}$$

where

$$\Pi(n,m) = \int_0^{\pi/2} \frac{\mathrm{d}t}{[1 - n\sin^2 t][1 - m\sin^2 t]^{1/2}} \tag{3.20}$$

is the complete elliptic integral of the third kind.

Upon using (3.16) and (3.19), (3.15a) can be rewritten as

$$\zeta = H(1 - 1/n)\left\{\Pi(n,m)/\mathrm{K}(m) - \left[1 - n\mathrm{sn}^2\left(\frac{2\mathrm{K}}{\Lambda}\bar{\phi} + \Phi_0\right)\right]^{-1}\right\}. \tag{3.21}$$

Given H (wave height), Λ (wavelength) and θ_0 (angle of incidence), we first express n in terms of m through (3.15c) and (3.16):

$$n = n_{\pm} = \frac{1}{2}\left[(m + \Gamma) \pm \sqrt{(m+\Gamma)^2 - 4\Gamma}\right], \tag{3.22a}$$

where

$$\Gamma(m) = \frac{1}{32\mathrm{K}^2(m)}\left(H\Lambda/\cos\theta_0\right)^2. \tag{3.22b}$$

Note that since n $(0 < n < 1)$ is a real parameter, the range of m is a subset of (0,1) such that the determinant $[(m+\Gamma)^2 - 4\Gamma] \geq 0$. Substituting (3.22) into (3.19), we obtain a transcendental equation for m. It can be showed that for $r < 0 (r > 0)$, no solution can be found when $n = n_+ (n = n_-)$ is substituted into (3.19), whereas a unique solution is obtained when $n = n_- (n = n_+)$ is substituted. Indeed, for the same value of m, if (m, n_-) corresponds to (ζ, r), then (m, n_+) should correspond to $(-\zeta, -r)$ with a phase shift $\mathrm{K}(m)$. The reason is that (3.9) is invariant under transformation $(\zeta, r) \mapsto (-\zeta, -r)$.

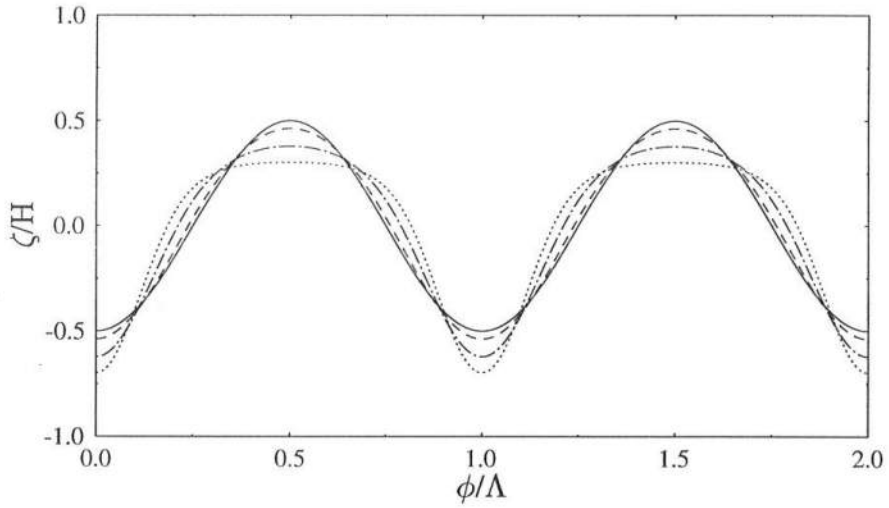

Figure 1. Profiles of the periodic wave (3.21) for different values of P_1 with $P_2 = -0.5$: (- - - -), $P_1 = 5.0$ $(m = 0.7229, n = 0.2869)$; $(- \cdot -)$, $P_1 = 10.0$ $(m = 0.9549, n = 0.3856)$; $(\cdots)$, $P_1 = 15.0$ $(m = 0.9943, n = 0.4507)$. For comparison, the sinusoidal wave profile (3.24) is also plotted in this figure (——).

From (3.19) and (3.22), one can see that the normalized wave profile corresponding to (3.21), i.e. ζ/H as a function of $\bar{\phi}/\Lambda$, actually only depends on two combined parameters $P_1 = H\Lambda/\cos\theta_0$ and $P_2 = r/H$. The shapes of the periodic wave given by (3.21) for different values of P_1 with fixed P_2 are shown in figure 1, whereas the shapes of the periodic wave for different values of P_2 with the same P_1 are plotted in figure 2.

For every case, the corresponding values of m and n are given in the parentheses. For fixed $P_2 < 0$, both m and n increase as P_1 increases (see the caption of figure 1). On the other hand, for the same P_1, m increases but n decreases as $|P_2|$ increases (see the caption of figure 2). When $r < 0$ (i.e. $P_2 < 0$), as P_1 or $|P_2|$ increases, the wave crest becomes flatter, whereas the trough becomes steeper. When $r > 0$, the situation is just opposite because the crest becomes the trough and vice versa under transformation $(\zeta, r) \mapsto (-\zeta, -r)$. Two limiting cases: $m \to 1$ and $m \to 0$ are discussed as follows.

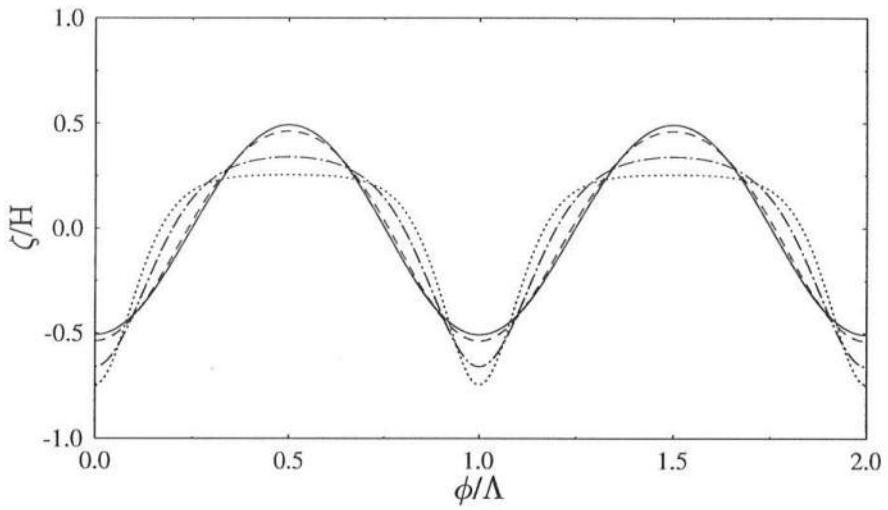

Figure 2. Profiles of the periodic wave (3.21) for different values of P_2 with $P_1 = 5.0$: (——), $P_2 = -0.1$ $(m = 0.6799, n = 0.3987)$; (- - - -), $P_2 = -0.5$ $(m = 0.7229, n = 0.2869)$; $(-\cdot-)$, $P_2 = -2.5$ $(m = 0.9523, n = 0.0960)$; $(\cdots)$, $P_2 = -5.0$ $(m = 0.9942, n = 0.0499)$.

(a) $m \to 1$. In this limit, the wavelength Λ becomes infinite long according to (3.16) (the close orbit in the (χ, ϑ)-plane becomes a homoclinic orbit, as shown in figure A1), but $2\mathrm{K}(m)/\Lambda \to H \sec\theta_0/\sqrt{8n}$. It can be readily shown that $\mathrm{sn}(\Phi, m) \to \tanh\Phi$, $\Pi(n, m)/\mathrm{K}(m) \to 1/(1-n)$, and from (3.19) $H \to -4nr/(1+n)$. In this situation, the

periodic-wave solution (3.21) reduces to the solitary-wave solution:

$$\zeta = \left(\frac{4rn}{1+n}\right)\frac{\operatorname{sech}^2\Phi}{1-n\tanh^2\Phi}, \quad \Phi = K\bar{X} + K\tan\theta_0\bar{Y} - \Omega\bar{T} + \Phi_0, \tag{3.23a}$$

with

$$K = \frac{|r|}{1+n}(2n)^{1/2}, \qquad \Omega = 4K^3 + 3K\tan^2\theta_0. \tag{3.23b}$$

Note that the height of the solitary wave given by (3.23) increases as n increases and has an upper bound $|2r|$.

(b) $m \to 0$. In this limit, $n, H \to 0$; the periodic wave becomes infinitesimal. As $m, n \to 0$, $\mathrm{sn}(\Phi, m) \to \sin\Phi$, $\mathrm{K}(m) \to \pi/2$, and $\Pi(n,m)/\mathrm{K}(m) \to (1 + n/2)$, (3.21) reduces to

$$\zeta = -\frac{H}{2}\cos\left[\frac{2\pi}{\Lambda}(\cos\theta_0\bar{X} + \sin\theta_0\bar{Y} - V\bar{T}) + \Phi_0\right], \tag{3.24a}$$

where

$$V = \cos\theta_0(3\tan^2\theta_0 - 4\pi^2\cos^2\theta_0/\Lambda^2). \tag{3.24b}$$

We remark that (3.24) is the sinusoidal-wave solution for the linearized equation of (3.9).

The second family of periodic solutions to (3.9) is given by

$$\zeta = r + \tfrac{1}{2}H\mathrm{sn}(\Phi, m), \tag{3.25a}$$

with

$$\Phi = K\sec\theta_0\bar{\phi} + \Phi_0 = K\sec\theta_0\left(\cos\theta_0\bar{X} + \sin\theta_0\bar{Y} - V\bar{T}\right) + \Phi_0, \tag{3.25b}$$

$$K = H/(2\sqrt{2}\,m), \tag{3.25c}$$

$$V = \cos\theta_0\left\{3r^2 + 3\tan^2\theta_0 - \tfrac{1}{8}H^2(1/m^2 + 1)\right\}, \tag{3.25d}$$

where H is the wave height, m $(0 < m < 1)$ is the modulus of the snoidal wave, K is the $\bar{X}$-component wavenumber, V is the phase speed, θ_0 is the angle of incidence and Φ_0 is a phase constant. The wavelength of the snoidal wave Λ is given by

$$\Lambda = 4\mathrm{K}(m)\cos\theta_0/K = 8\sqrt{2}\,m\mathrm{K}(m)\cos\theta_0/H. \tag{3.26}$$

Upon using (3.26), (3.25a) can be rewritten as

$$\zeta = r + \tfrac{1}{2} H \mathrm{sn}\left(\frac{4\mathrm{K}}{\Lambda}\bar{\phi} + \Phi_0\right). \tag{3.27}$$

Given H, Λ and θ_0, or more compactly, given $P_1 = H\Lambda/\cos\theta_0$, m can be uniquely determined from (3.26). Note that the mean interface corresponding to the snoidal wave (3.27) is located at $z = r$. Unlike the wave profiles of the first family of periodic waves (see figures 1 and 2), the profiles of the second family of periodic waves are symmetric about its mean interface location. Figure 3 shows the profiles of the snoidal wave (3.27) for different values of P_1. The corresponding values of m are given in the parentheses. One can see that as P_1 increases, m increases, and the wave crest and trough both become flatter and broader. Two limiting cases corresponding to $m \to 1$ and $m \to 0$ are discussed below.

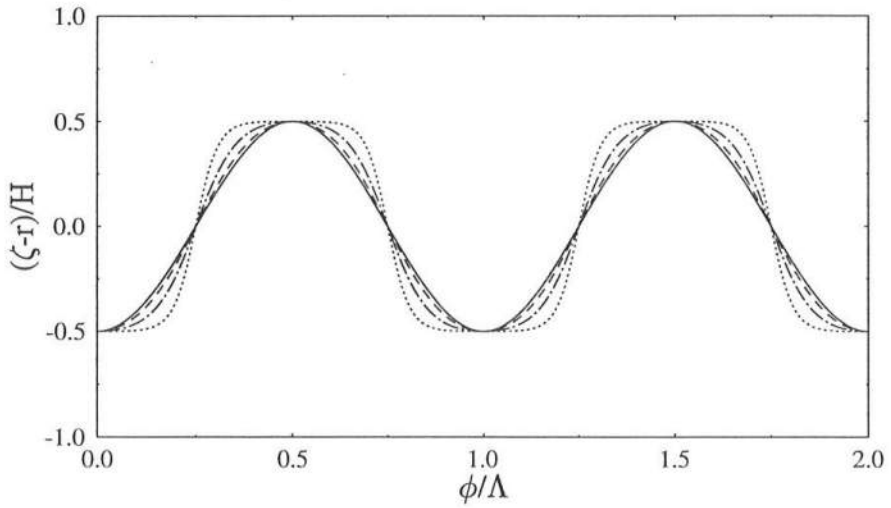

Figure 3. Profiles of the periodic wave (3.27) for different values of P_1 with $\Phi_0 = -\mathrm{K}(m)$: (- - - -), $P_1 = 10.0$ ($m = 0.4808$); (— · —), $P_1 = 25.0$ ($m = 0.8827$); (· · · ·), $P_1 = 50.0$ ($m = 0.9977$). For comparison, the sinusoidal wave profile (3.29) is also plotted in this figure (——).

(a) $m \to 1$. In this limit, the wavelength of the snoidal wave becomes infinite long (the close orbit in the (χ, ϑ)-plane becomes a heteroclinic orbit (see figure A2)), but $4\mathrm{K}(m)/\Lambda \to H \sec\theta_0/\sqrt{8}$. By further imposing $\zeta \to 0$ as $\Phi \to +\infty$, we obtain the isolated shock-like solution to (3.9), which is

$$\zeta = r[1 - \tanh\Phi], \qquad \Phi = K\bar{X} + K\tan\theta_0\bar{Y} - \Omega\bar{T} + \Phi_0, \tag{3.28a}$$

where

$$K = |r|/\sqrt{2}, \qquad \Omega = 4K^3 + 3K\tan^2\theta_0. \tag{3.28b}$$

Since (3.9) is invariant under transformation $\zeta \mapsto 2r - \zeta$, from (3.28), we have $\zeta = r[1 + \tanh\Phi]$, which is the isolation shock-like solution satisfying $\zeta \to 0$ as $\Phi \to -\infty$. For definiteness, we assume that $\zeta \to 0$ as $\Phi \to +\infty$.

(b) $m \to 0$. In this limit, $H \to 0$. The snoidal wave (3.27) becomes an infinitesimal sinusoidal wave:

$$\zeta = r + \frac{H}{2}\sin\left[\frac{2\pi}{\Lambda}(\cos\theta_0\bar{X} + \sin\theta_0\bar{Y} - V\bar{T}) + \Phi_0\right], \tag{3.29a}$$

with

$$V = \cos\theta_0\left(3r^2 + 3\tan^2\theta_0 - 4\pi^2\cos^2\theta_0/\Lambda^2\right). \tag{3.29b}$$

It is easy to show that (3.29) indeed is the sinusoidal-wave solution for the equation obtained by linearized (3.9) about $\zeta = r$.

Note that the dependent variable transformation (3.8a) does not include any of the new or old independent variables. Thus, on substitution of (3.8) into (3.21), (3.27) and (3.23), (3.28), we obtain the corresponding periodic-wave solutions, solitary-wave solutions and a shock-like solution (satisfying $\eta_0 \to 0$ as $\xi \to +\infty$), to the variable-coefficient equation (3.7). The phase Φ of these waves can be expressed as

$$\begin{aligned}\Phi \;=\; & \sqrt{6}K\left\{\xi + Y\left[(6D_1)^{1/2}\tan\theta_0/C - \int_0^X F_1(q)\mathrm{d}q\right] - \int_0^X\left[\Omega D_1/(CK)\right.\right. \\ & + \left.\left. F_0(q) - (6D_1)^{1/2}\tan\theta_0\int_0^q F_1(s)\mathrm{d}s + \frac{C}{2}\left(\int_0^q F_1(s)\mathrm{d}s\right)^2\right]\mathrm{d}q\right\} + \Phi_0. \end{aligned} \tag{3.30}$$

In the moving coordinates (ξ, X, Y), at different X, the lines of constant phase remain straight parallel lines in the (ξ, Y)-plane. However, their direction will change due to the contribution from F_1, whose relation with the topography is described by (3.6). The contribution from F_0 only causes the lines of constant phase to translate and hence changes the speed of the wave in the moving coordinates.

To save the space, only the explicit expressions for the family of the solitary-wave solutions and the isolated shock-like solution are given here. The expression for the family of solitary-wave solutions to (3.7) is

$$\eta_0 = \left[\frac{D_{-2}n}{\alpha\mu D_{-3}(1+n)}\right]\frac{\operatorname{sech}^2\Phi}{1-n\tanh^2\Phi}, \tag{3.31a}$$

where Φ is given by (3.30) with

$$K = \frac{C|D_{-2}|}{4\mu(1+n)}\left(\frac{2n}{D_1 D_{-3}}\right)^{1/2}, \quad \Omega = 4K^3 + 3K\tan^2\theta_0. \tag{3.31b}$$

The expression for the shock-like solution to (3.7) is

$$\eta_0 = \frac{D_{-2}[1-\tanh\Phi]}{4\alpha\mu D_{-3}}, \tag{3.32a}$$

where Φ again is given by (3.30) with

$$K = \frac{C|D_{-2}|}{4\mu(2D_1 D_{-3})^{1/2}}, \quad \Omega = 4K^3 + 3K\tan^2\theta_0. \tag{3.32b}$$

Note that when $D_{-2} = 0 (r = 0)$, i.e. exactly at the critical depth level, we have only trivial solution $\eta_0 = 0$ which vanishes at infinity.

If the sidewalls are given by

$$Y_R(X) = \int_0^X \left[(6D_1)^{1/2}\tan\theta_0 - C\int_0^q F_1(s)\mathrm{d}s\right]\mathrm{d}q + Y_R(0), \tag{3.33a}$$

$$Y_L(X) = \int_0^X \left[(6D_1)^{1/2}\tan\theta_0 - C\int_0^q F_1(s)\mathrm{d}s\right]\mathrm{d}q + Y_L(0), \tag{3.33b}$$

any travelling-wave solution $\zeta = \zeta(\bar{X} + \tan\theta_0\bar{Y} - \omega\bar{T})$ will satisfy boundary conditions (3.11). Thus, for those sidewalls given by (3.33) (note that they are parallel), the

periodic-wave solutions we have found, including the family of solitary-wave solutions (3.31) and the isolated shock-like solution (3.32), automatically satisfy boundary conditions (2.12) with $\gamma = 0$.

In summary, in the absence of rotation, we have obtained analytic expressions to describe transformations of two different types of interfacial periodic waves (asymmetric and symmetric about the mean interface location) propagating near the critical depth level and over a weak topography with linear transverse variation. When the wavelength becomes infinite, these expressions reduce to (3.31) and (3.32), which describe the propagations of interfacial concave ($D_{-2} < 0$) or convex ($D_{-2} > 0$) solitary waves and a non-dissipative jump ($D_{-2} < 0$) or bore ($D_{-2} > 0$) in the same setting, respectively. The presence of the sidewalls usually will interfere with the propagations of these finite-amplitude waves, but for those parallel sidewalls given by (3.33), the presence of the sidewalls will not affect the wave propagations. The most striking feature is that these three-dimensional waves can remain intact in certain type of curved channels with varying topography; the only changes are the propagation directions and the phase speeds.

Finally, for an incident Kelvin solitary wave given by

$$\eta_0(\xi, 0, Y) = \left[\frac{D_{-2}n}{\alpha\mu D_{-3}(1+n)}\right] \frac{\operatorname{sech}^2\left\{\sqrt{6}K[\xi + (6D_1)^{1/2}\tan\theta_0 Y/C]\right\}\exp(-\beta Y/C)}{1 - n\tanh^2\left\{\sqrt{6}K[\xi + (6D_1)^{1/2}\tan\theta_0 Y/C]\right\}}, \tag{3.34}$$

propagating in a varying channel, assuming that the solution evolved from this initial condition is locally confined ((3.34) satisfies (2.18) at $X = 0$), we obtain explicit expressions for the first-order and second-order invariants $\mathcal{I}$ ($\beta = 0$) and $\mathcal{J}$ (see (2.16) and (2.17)), which are

$$\mathcal{I} = \operatorname{sign}(\mathrm{D}_{-2})\frac{2}{\alpha}(W/C)^{1/2}\left(\frac{D_1}{3D_{-3}}\right)^{1/2}\ln\frac{1+n^{1/2}}{1-n^{1/2}} \qquad (\beta = 0), \tag{3.35a}$$

$$\mathcal{J} = \left(\frac{D_1}{3D_{-3}}\right)^{1/2}\frac{|D_{-2}|}{\alpha^2\mu D_{-3}}\left(-\frac{n^{1/2}}{1+n} + \frac{1}{2}\ln\frac{1+n^{1/2}}{1-n^{1/2}}\right)$$

$$\times \frac{C}{\beta} \left[\exp\left(-2\beta Y_R/C\right) - \exp\left(-2\beta Y_L/C\right) \right], \tag{3.35b}$$

where all the functions are evaluated at X=0. These two analytic expressions are useful to test the accuracy of numerical schemes for (2.11) and (2.12).

4. Kelvin solitary wave propagation in a rotating uniform channel

Using the rotation-modified KP (rmKP) equation, Katsis & Akylas (1987) and Grimshaw & Tang (1990) investigated the rotation effect on the evolution of an initially straight-crested Kelvin solitary wave in a uniform channel. They confirmed that the rotation gives rise to a solitary-like wave whose wavefront is curved back, which is in qualitative agreement with the experiments of Maxworthy (1983) and Renouard, Chabert d'Hiéres & Zhang (1987). Katsis & Akylas' numerical results also showed that the wave amplitude decays slowly as the disturbance propagates downstream. This indicates that the solitary-like wave is not a wave of permanent form and the observed attenuation in experiments is only partly caused by the viscous damping. By studying a coupled set of evolution equations, which are asymptotically equivalent to the rmKP equation, Melville *et al.* (1989) explained that the backward curvature and the attenuation along the channel are caused by resonant interactions between the nonlinear Kelvin wave and linear Poincaré waves, which are generated by resonant forcing of the Kelvin wave. Similar conclusion was also reached by Grimshaw & Tang (1990) using a small-time asymptotic analysis of the rmKP equation.

In this section, we study Kelvin solitary wave propagation near the critical depth level in a rotating uniform channel to examine the effect of the cubic nonlinearity on the wave propagation. Following Grimshaw & Tang (1990), we first carry out the small-time asymptotic analysis for (2.11) with constant coefficients and then numerically solve the equation. We shall show that depending on the relative importance of the

cubic nonlinearity to quadratic nonlinearity, an initially straight-crested Kelvin solitary wave can curve backwards or forwards, or remain almost straight-crested as the wave propagates down the channel.

To compare with the results obtained by Grimshaw & Tang (1990), we introduce the following transformation:

$$\eta_0 = \frac{2\mu^2}{\epsilon C^2 D_{-2}}(D_1/3)^{1/2}u, \quad X = 2C\,(3/D_1)^{1/4}\,\tau, \quad \xi = (D_1/3)^{1/4}\theta, \quad Y = C\lambda, \tag{4.1}$$

which transforms (2.11) and (2.12) (with $Y_R = 0, Y_L = W$) for waves propagating in a rotating uniform channel into

$$\frac{\partial^2 u}{\partial\tau\partial\theta} + 3\frac{\partial^2 u^2}{\partial\theta^2} - P\frac{\partial^2 u^3}{\partial\theta^2} + \frac{\partial^4 u}{\partial\theta^4} + \frac{\partial^2 u}{\partial\lambda^2} - \beta^2 u = 0, \tag{4.2}$$

$$\frac{\partial u}{\partial\lambda} + \beta u = 0, \quad \text{on } \lambda = 0, l \tag{4.3}$$

where

$$P = \frac{8\mu^2 D_{-3}}{C^2 D_{-2}^2}(D_1/3)^{1/2} > 0, \quad l = W/C. \tag{4.4}$$

Note that the rmKP equation studied by Grimshaw & Tang (1990) did not include the cubic nonlinearity. Equation (4.2) recovers their equation if $P = 0$.

It is easy to show that the following transverse modal functions, satisfying the boundary conditions (4.3), form a complete and orthogonal set

$$\phi_0(\lambda) = \exp(-\beta\lambda), \tag{4.5a}$$

$$\phi_n(\lambda) = \cos\frac{n\pi}{l}\lambda - \frac{\beta l}{n\pi}\sin\frac{n\pi}{l}\lambda, \quad n = 1, 2, \ldots. \tag{4.5b}$$

The mode $n = 0$ is the Kelvin wave mode and the remaining modes ($n \geq 1$) are Poincaré wave modes. We now expand the solution of (4.2) in the form

$$u(\theta, \tau, \lambda) = A_0(\theta, \tau)\exp(-\beta\lambda) + B(\theta, \tau, \lambda), \tag{4.6a}$$

where

$$B(\theta, \tau, \lambda) = \sum_{n=1}^{\infty} A_n(\theta, \tau)\phi_n(\lambda) \tag{4.6b}$$

represents all the Poincaré modes. Suppose that initially only the Kelvin wave component exists, i.e. $B = 0$ at $\tau = 0$. So B can be expected to remain small in sufficiently small 'time' τ. On substitution of (4.6) into (4.2) and (4.3), and with the use of orthogonality, for small τ, the governing equations for Kelvin wave component and Poincaré wave component can be approximated by

$$\begin{aligned}\frac{\partial A_0}{\partial \tau} &+ 3\frac{a_3}{a_2}\frac{\partial A_0^2}{\partial \theta} - P\frac{a_4}{a_2}\frac{\partial A_0^3}{\partial \theta} + \frac{\partial^3 A_0}{\partial \theta^3} + \frac{6}{a_2}\frac{\partial}{\partial \theta}\left(A_0\int_0^l Be^{-2\beta\lambda}\mathrm{d}\lambda\right) \\ &- \frac{3P}{a_2}\frac{\partial}{\partial \theta}\left(A_0^2\int_0^l Be^{-3\beta\lambda}\mathrm{d}\lambda\right) = O(B^2), \end{aligned} \tag{4.7}$$

and

$$\begin{aligned}\frac{\partial^2 B}{\partial \tau \partial \theta} &+ \frac{\partial^4 B}{\partial \theta^4} + \frac{\partial^2 B}{\partial \lambda^2} - \beta^2 B + 6e^{-\beta\lambda}\frac{\partial^2}{\partial \theta^2}\left[A_0\left(B - \frac{1}{a_2}\int_0^l Be^{-2\beta\lambda}\mathrm{d}\lambda\right)\right] \\ &- 3Pe^{-\beta\lambda}\frac{\partial^2}{\partial \theta^2}\left[A_0^2\left(Be^{-\beta\lambda} - \frac{1}{a_2}\int_0^l Be^{-3\beta\lambda}\mathrm{d}\lambda\right)\right] \\ &= -3e^{-\beta\lambda}\left(e^{-\beta\lambda} - \frac{a_3}{a_2}\right)\frac{\partial^2 A_0^2}{\partial \theta^2} + Pe^{-\beta\lambda}\left(e^{-2\beta\lambda} - \frac{a_4}{a_2}\right)\frac{\partial^2 A_0^3}{\partial \theta^2} + O(B^2), \end{aligned} \tag{4.8a}$$

$$\frac{\partial B}{\partial \lambda} + \beta B = 0, \qquad \text{on } \lambda = 0, l, \tag{4.8b}$$

respectively, where

$$a_n = \int_0^l e^{-n\beta\lambda}\mathrm{d}\lambda = \frac{1}{n\beta}\left(1 - e^{-n\beta l}\right). \tag{4.9}$$

From (4.8a), it is clear that an initially straight-crested Kelvin solitary wave cannot maintain its original shape, because it will generate the Poincaré waves through resonant forcing (Melville *et al.* 1989), which will further interact with the Kelvin wave component.

To the leading order, (4.7) for the Kelvin wave component becomes

$$\frac{\partial A_0}{\partial \tau} + 3\frac{a_3}{a_2}\frac{\partial A_0^2}{\partial \theta} - P\frac{a_4}{a_2}\frac{\partial A_0^3}{\partial \theta} + \frac{\partial^3 A_0}{\partial \theta^3} \approx 0, \tag{4.10}$$

which has a solitary-wave solution:

$$A_0(\theta, \tau) \approx S(\theta, \tau) = \frac{a\,\mathrm{sech}^2\Phi}{1 - \Upsilon\tanh^2\Phi}, \quad \Phi = k(\theta - 4k^2\tau), \tag{4.11a}$$

where

$$\Upsilon = \frac{aPa_4}{4a_3 - aPa_4}, \quad k = \frac{1}{2}\sqrt{\frac{a}{2a_2}(4a_3 - aPa_4)}, \tag{4.11b}$$

and a $(0 < a < 2a_3/Pa_4)$ is the amplitude of the solitary wave. Since we have assumed that $B = 0$ at $\tau = 0$, it follows from (4.8) that for small enough τ, the Poincaré waves generated by the Kelvin solitary wave can be expressed as

$$B = -\tau e^{-\beta\lambda}\left[3\frac{\partial S^2}{\partial\theta}\left(e^{-\beta\lambda} - \frac{a_3}{a_2}\right) - P\frac{\partial S^3}{\partial\theta}\left(e^{-2\beta\lambda} - \frac{a_4}{a_2}\right)\right] + O(\tau^2). \tag{4.12}$$

Note that (4.12) satisfies the boundary conditions (4.8b) (up to $O(\tau^2)$), because

$$e^{-2\beta\lambda} - \frac{a_3}{a_2}e^{-\beta\lambda} = \sum_{n=1}^{\infty}\phi_n(\lambda)\left[\int_0^l \phi_n(\lambda)e^{-2\beta\lambda}\mathrm{d}\lambda \Big/ \int_0^l \phi_n^2(\lambda)\mathrm{d}\lambda,\right], \tag{4.13a}$$

$$e^{-3\beta\lambda} - \frac{a_4}{a_2}e^{-\beta\lambda} = \sum_{n=1}^{\infty}\phi_n(\lambda)\left[\int_0^l \phi_n(\lambda)e^{-3\beta\lambda}\mathrm{d}\lambda \Big/ \int_0^l \phi_n^2(\lambda)\mathrm{d}\lambda\right]. \tag{4.13b}$$

Substituting (4.12) into (4.7), we find that

$$\begin{aligned}\frac{\partial A_0}{\partial\tau} &+ 3\frac{a_3}{a_2}\frac{\partial A_0^2}{\partial\theta} - P\frac{a_4}{a_2}\frac{\partial A_0^3}{\partial\theta} + \frac{\partial^3 A_0}{\partial\theta^3} - \frac{\tau}{a_2}\left[12(a_4 - a_3^2/a_2)\frac{\partial^2 S^3}{\partial\theta^2}\right.\\ &- \left. 9P(a_5 - a_3a_4/a_2)\frac{\partial^2 S^4}{\partial\theta^2} + \frac{9}{5}P^2(a_6 - a_4^2/a_2)\frac{\partial^2 S^5}{\partial\theta^2}\right] = O(\tau^2).\end{aligned} \tag{4.14}$$

The solution to (4.14), correcting up to $O(\tau^3)$, is given by

$$\begin{aligned}A_0 = S &+ \frac{\tau^2}{2a_2}\left[12(a_4 - a_3^2/a_2)\frac{\partial^2 S^3}{\partial\theta^2} - 9P(a_5 - a_3a_4/a_2)\frac{\partial^2 S^4}{\partial\theta^2}\right.\\ &+ \left.\frac{9}{5}(a_6 - a_4^2/a_2)P^2\frac{\partial^2 S^5}{\partial\theta^2}\right] + O(\tau^3).\end{aligned} \tag{4.15}$$

Substituting (4.15) and (4.12) into (4.6a), we find that the solution to (4.2) and (4.3), correcting up to $O(\tau^2)$, can be written as

$$u = \frac{a\,\mathrm{sech}^2\left\{k[\theta - 4k^2\tau - V_1(\theta,\lambda)\tau]\right\}}{1 - \Upsilon\tanh^2\left\{k[\theta - 4k^2\tau - V_1(\theta,\lambda)\tau]\right\}}e^{-\beta\lambda} + O(\tau^2), \tag{4.16}$$

where

$$V_1(\theta,\lambda) = 6S(\theta,0)\left(e^{-\beta\lambda} - \frac{a_3}{a_2}\right) - 3S^2(\theta,0)P\left(e^{-2\beta\lambda} - \frac{a_4}{a_2}\right), \tag{4.17}$$

which can be interpreted as a correction to the incident wave speed $V = 4k^2$ due to the Poincaré waves (4.12). Note that when $P = 0$, the above results agree with the corresponding results obtained by Grimshaw & Tang (1990).

There are two terms in (4.17). The first term comes from the quadratic nonlinearity, whereas the second term comes from the cubic nonlinearity. At the wall $\lambda = 0$, the first term is positive, whereas the second term is negative (note that $P > 0$). As λ increases, the first term decreases and becomes negative at the other wall $\lambda = l$ (assuming $\beta > 0$), whereas the second term behaves just opposite. Therefore, the cubic nonlinearity tends to cause the wavefront, which is initially straight-crested in the transverse direction, to curve forwards relative to the wall where it initially has the largest amplitude (here $\lambda = 0$ for $\beta > 0$), whereas the quadratic nonlinearity tends to cause the wavefront to curve backwards. For waves propagating near the critical depth level, both the quadratic and cubic nonlinearities are equally important. The combined effect on the curvature of the wavefront depends on the ratio of the first term to the second term in (4.17). From (4.2) and (4.10), one can see that in the (τ, θ, λ) coordinates, for fixed incident wave amplitude a, rotation rate β and channel width l, the relative importance of the cubic nonlinearity to the quadratic nonlinearity can be simply measured by the parameter P. Figure 4 shows the variation of the relative speed correction along the crest line ($\theta = 0$), $V_1(0, \lambda)/V$, across a channel for a Kelvin solitary wave given by (4.11) for different values of P with $a = 2.0, \beta = 1.0$ and $l = 1.25$. The corresponding mean-squared relative speed correction $l^{-1} \int_0^l [V_1(0, \lambda)/V]^2 \mathrm{d}\lambda$ achieves its minimum value at $P_o = 0.791$ and increases as $|P - P_o|$ increases. Note that for the given a and βl, there is a upper limit for P, which is $2a_3/(aa_4) = 1.31$. As P gets close to this upper limit, the solitary wave (4.11) becomes broader and flatter. From figure 4 and the behavior of the mean-squared relative speed correction along the crest line as P varies, one can expect that for small value of P, the quadratic nonlinearity dominates the cubic nonlinearity and the Poincaré waves generated by the Kelvin solitary wave will cause the wavefront

to curve backwards, whereas for large value of P, the cubic nonlinearity dominates the quadratic nonlinearity and the wavefront will curve forwards. For some intermediate value of P (near P_o), the contributions from the quadratic and cubic nonlinearity almost balance each other and the Poincaré waves generated by the Kelvin solitary wave are very weak. As a result, the speed correction due to the Poincaré waves is not significant, as indicated by the dotted line in figure 4. In this situation, the wavefront almost remains straight-crested across the channel.

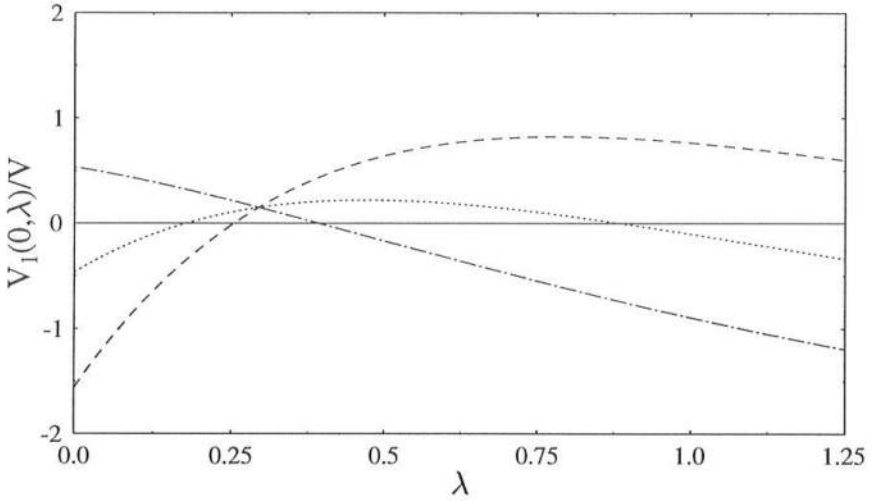

Figure 4. A plot of $V_1(0,\lambda)/V$ as a function of λ for different values of P: $(- \cdot -)$, $P = 0.4$; $(\cdots)$, $P = 0.8$; and (- - -), $P = 1.1$.

The above analysis is valid only for small 'time' τ. To see if the prediction is also applied to finite τ, we numerically solve (4.2) with (4.3). The numerical scheme developed by Chen & Liu (1996*b*) for the uKP equation is modified to solve (4.2) with (4.3). The incident Kelvin solitary wave is given by (4.11) with $a = 2.0, \beta = 1.0$ and $l = 1.25$ (unless otherwise noted), which satisfies the constraint $\int_{-\infty}^{\infty} u d\theta = F(\tau)\exp(-\beta\lambda)$ at $\tau = 0$. In the numerical computations, $\Delta\theta = 0.2$, $\Delta\lambda = 0.05$, and $\Delta\tau = 0.25 \times 10^{-3}$ has been used. In each of the numerical examples given below, the relative errors between

the numerically evaluated second-order integral invariant and its exact value at different τ are never in excess of 0.5%.

For small time τ, we find that the numerical results agree very well with the predictions given by (4.16) and (4.17). Figure 5 shows the contour plots of $u(\tau, \theta, \lambda)$ at finite time $\tau = 1.5$ for different values of P: 0.4, 0.8 and 1.1. The numerical results show that at finite time, the curvature of the wavefronts is consistent with the predictions based on the small-time analysis. For small value of P (see figure 5*a*), the quadratic nonlinearity is dominant; the wave pattern looks very similar to that described by the rmKP equation (i.e. $P = 0$). The curved-back front moves as a whole and is trailed by a train of small-amplitude Poincaré waves, which is dominated by its first mode (see figure 5*a*). The maximum wave amplitude attenuates gradually along the sidewall ($\lambda = 0$) as the disturbance propagates downstream (see dashed-dotted line in figure 6). As the rotation rate increases, the extent of the wavefront curvature and the amplitude of the trailing Poincaré waves both increase. For large value of P (see figure 5*c*), the cubic nonlinearity is dominant; the wavefront curves forwards, accompanied by a smaller Poincaré wave train (compared with those associated with small P value; cf. figure 5*a* with 5*c*). The maximum wave amplitude along the channel almost remains constant (see dashed line in figure 6). For $P = 0.8$, the wavefront is almost straight-crested across the channel, with very small trailing Poincaré waves (see figure 5*b*). Note that the leading wave is nearly symmetric about the crest line. The maximum wave amplitude along the channel decreases at the beginning, but pretty soon reaches a constant value as shown in figure 6 (dotted line).

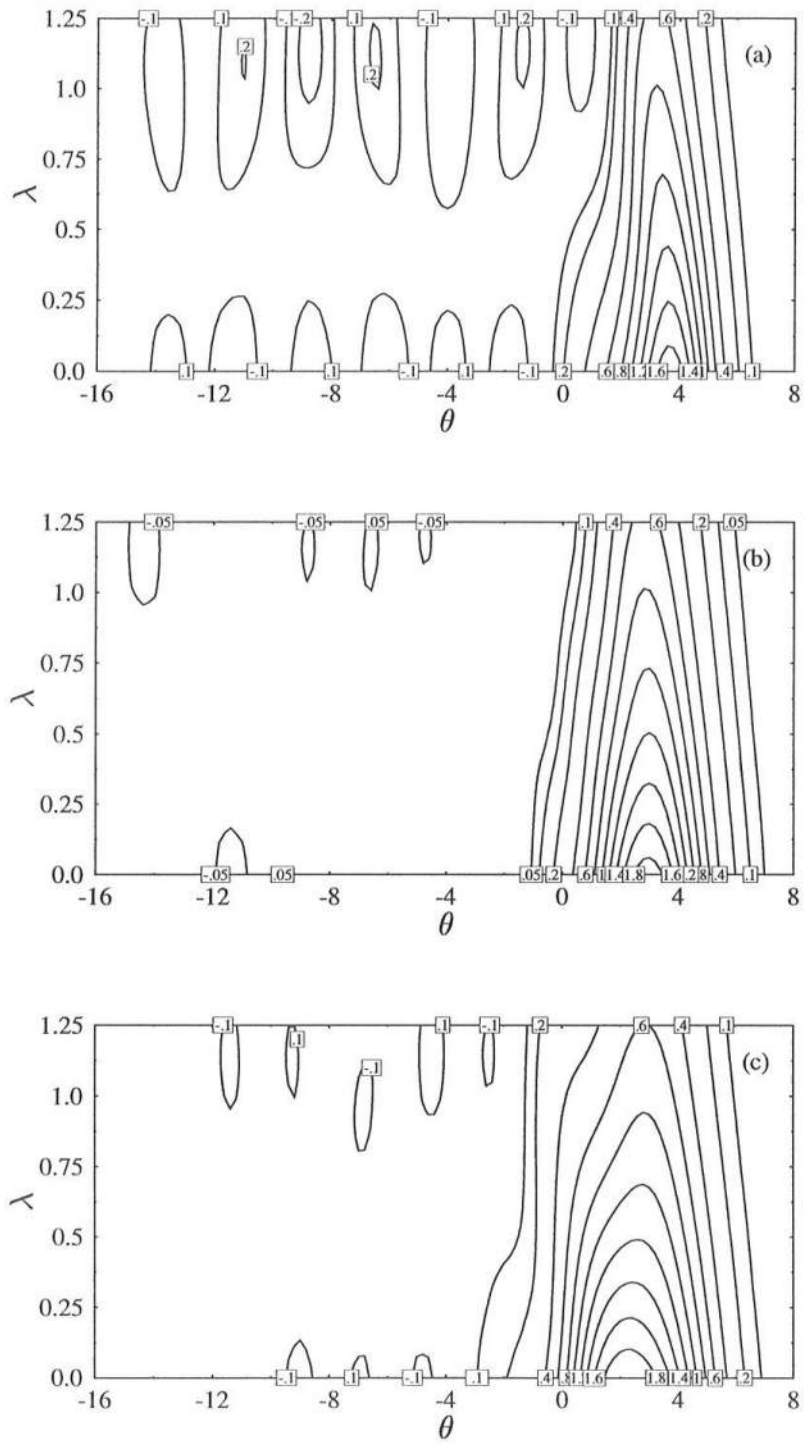

Figure 5. Contour plots of $u(\tau, \theta, \lambda)$ at $\tau = 1.5$ for different P values: (a) $P = 0.4$; (b) $P = 0.8$; (c) $P = 1.1$.

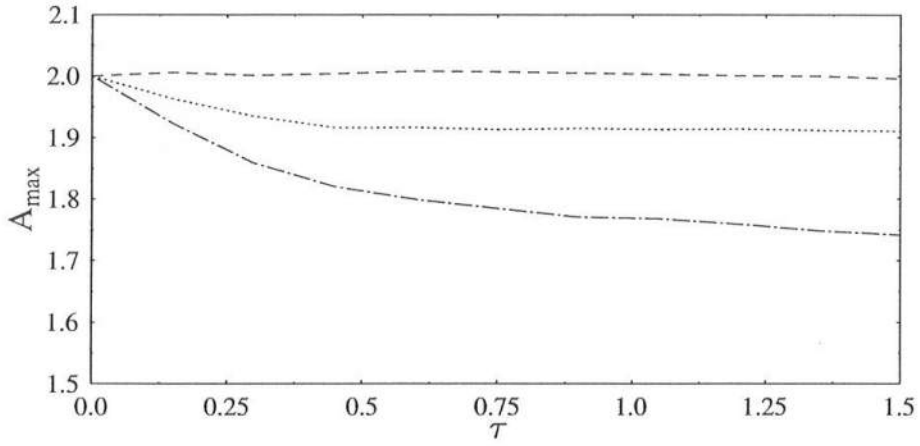

Figure 6. The variation of the maximum wave amplitude at the right-hand sidewall ($\lambda = 0$) along the channel for different P values: $(- \cdot -)$, $P = 0.4$; $(\cdots)$, $P = 0.8$; (- - -), $P = 1.1$.

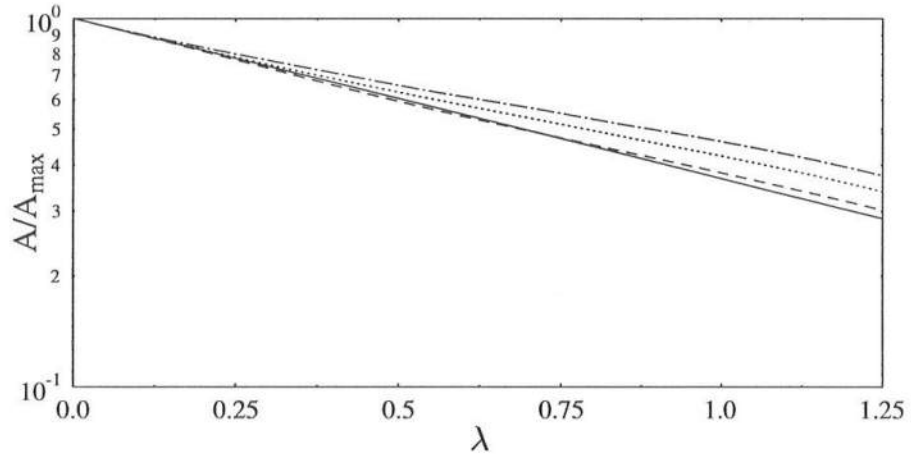

Figure 7. The decay of the amplitude of the leading wave at $\tau = 1.5$ across the channel along the wavecrest for different P values: $(- \cdot -)$, $P = 0.4$; $(\cdots)$, $P = 0.8$; (- - -), $P = 1.1$. For comparison, the liner Kelvin wave decay (——) is also shown.

Figure 7 shows the decay of the amplitude of the leading wave at $\tau = 1.5$ across the channel along the wavecrest for different P values. For comparison, the linear transverse

decay $\exp(-\beta\lambda)$ is also plotted in the figure (solid line). In each case, the broken line is very close to a straight line. This indicates that the variation of the wave amplitude along the wavecrest still remains exponential for a Kelvin solitary wave propagating near the critical depth level. As P increases, i.e. the cubic nonlinearity enhances, the decay rate increases and approaches to the linear decay rate. Note that for $P = 0.8$ case, since the leading wave is almost straight-crested and its maximum wave amplitude at $\tau = 1.5$ is smaller than that of the incident wave (see figure 6), the decay along the wavecrest should be slower than the linear decay owing to the conservation of energy. This is consistent with the results shown in figure 7 (cf. dotted line with solid line).

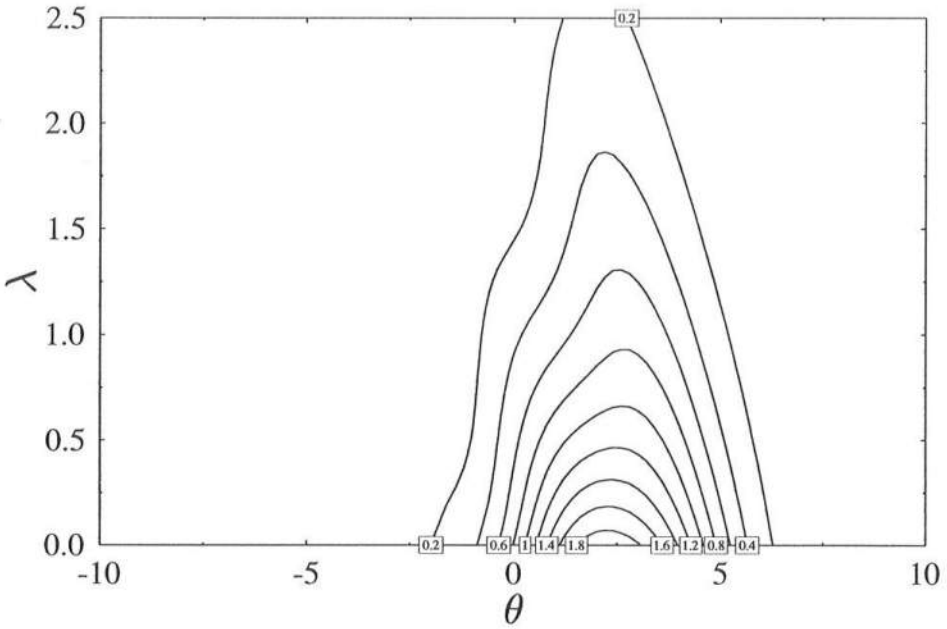

Figure 8. Contour plot of $u(\tau, \theta, \lambda)$ at $\tau = 1.5$ for $P = 1.1$ in a wider channel $\lambda = 2.5$ with $\beta = 1.0$ and $a = 2.0$.

Because Kelvin solitary waves exponentially decay across the channel, even if the cubic nonlinearity is dominant near the wall where it has the largest wave amplitude

(here $\lambda = 0$ for $\beta > 0$), the quadratic nonlinearity will dominate the cubic nonlinearity near the other wall if the channel is wide enough and/or the rotation is sufficiently fast. In this situation, the wavefront across the channel will first curve forwards and then curve backwards as clearly shown in figure 8.

5. Concluding remarks

Assuming that the effects of nonlinearity, dispersion, transverse modulation, rotation and variations of topography and sidewalls are weak but equally important, we have derived the evolution equation for three-dimensional interfacial wave propagation near the critical depth level, where the cubic nonlinearity is comparable to or dominates the quadratic nonlinearity in the parametric regime $O(\epsilon) = O(\mu)$. The resulting equation cannot pass the Painlevé PDE test due to the appearance of the cubic nonlinear term. Therefore, the search for analytical solutions becomes mathematically challenging. Under the same conditions as those for the uKP equation to be completely integrable (i.e. no rotation exists, the variation of topography is weak and behaves like a linear function in the transverse direction), we have found two families of periodic-wave solutions, expressed in terms of the snoidal function, to the variable-coefficient evolution equation. A family of solitary-wave solutions and an isolated shock-like solution, which may be regarded as a non-dissipative bore or jump, have also been obtained as the limiting cases of the periodic-wave solutions. The analytical solutions show that these finite-amplitude waves can remain intact in certain type of curved channels with varying topography. The integral invariants associated with the evolution equation for interfacial waves propagating in a varying channel have also been found and they turn out to be the same as those of the uKP equation.

Through the small-time asymptotic analysis and numerical study, we have found that depending on the relative importance of the cubic nonlinearity to quadratic nonlinearity, a straight-crested Kelvin solitary wave propagating in a rotating uniform

channel will curve backwards or forwards, trailed by a train of small Poincaré waves. When these two nonlinearities are almost in balance, the Kelvin wave remains almost straight-crested, with very small trailing Poincaré waves. The decay of the wave amplitude along the wavecrest across the channel remains almost exponential with the decay rate increasing as the cubic nonlinearity enhances. The maximum wave amplitude along the channel at the same location also increases as the cubic nonlinearity increases.

The effect of topographic variation on Kelvin solitary wave propagation near the critical depth level is under investigation and the results will be reported in the future.

Acknowledgments. This research was supported by a Mellon Foundation grant to the Center for Coastal Studies, Scripps Institution of Oceanography and by a grant from the Army Research Office (DAAL 03-92-G-0116) to Cornell University.

Appendix

In this appendix, we shall find all the bounded solutions to the set of equations

$$\frac{\mathrm{d}\chi}{\mathrm{d}\phi} = \vartheta, \qquad \frac{\mathrm{d}\vartheta}{\mathrm{d}\phi} = \chi^3 - p\chi + q, \tag{A1}$$

which is a conservative system and has the following first integral:

$$\tfrac{1}{2}(\chi')^2 - \tfrac{1}{4}(\chi^4 - 2p\chi^2 + 4q\chi) = \tfrac{1}{2}(\chi')^2 - f(\chi) = C, \tag{A2}$$

where $' = \mathrm{d}/\mathrm{d}\phi$, $f(\chi) = \frac{1}{4}(\chi^4 - 2p\chi^2 + 4q\chi)$ and C is the constant of integration. Since (A1) is invariant under transformation $(\chi, \vartheta, q) \mapsto (-\chi, -\vartheta, -q)$, without loss of generality, we can assume $q \geq 0$.

For the conservative system (A1), besides the equilibrium solutions, any other bounded solutions, if exist, correspond to close orbits in the phase plane (χ, ϑ). The existence of close orbits depends on the values of the parameters p and q. Carrying out analysis in the phase plane, we find out only when $p > 0$ and $0 \leq q < \frac{2}{3}p(p/3)^{1/2}$, there exist close orbits in the phase plane. Under these conditions, the cubic polynomial

$f'(\chi) = \chi^3 - p\chi + q = 0$ has three distinct real roots, denoted as α, β and γ with $\gamma < 0 \leq \beta < \alpha$, and system (A1) has three fixed points $(\alpha, 0)$, $(\beta, 0)$ and $(\gamma, 0)$, where $(\alpha, 0)$ and $(\gamma, 0)$ are saddle points and $(\beta, 0)$ is a center. The explicit expressions for the periodic solutions corresponding to the close orbits depend on whether q is equal to zero or not.

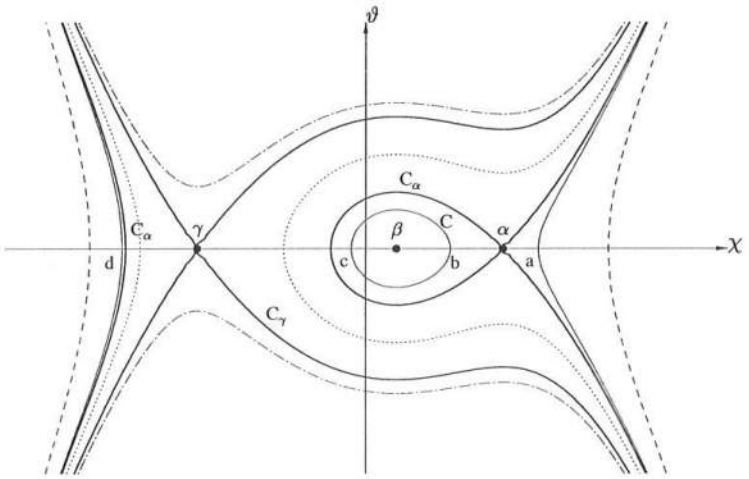

Figure A1: The phase portrait of system (A1) when $p > 0$ and $0 < q < \frac{2}{3}p(p/3)^{1/2}$.

(a) When $0 < q < \frac{2}{3}p(p/3)^{1/2}$, the phase portrait is shown in figure A1. If the constant of integration C in (A2) satisfies $-f(\alpha) = C_\alpha > C > C_\beta = -f(\beta)$, there exists a close orbit circling around the center $(\beta, 0)$. In this situation, $f(\chi) + C = 0$ has four distinct real roots: a, b, c and d, which satisfy $d < \gamma < c < \beta < b < \alpha < a$ (see figure A1). To obtain the periodic solution corresponding to close orbit C, we integrate the first integral (A2) along the close orbit and obtain

$$\int_c^\chi \frac{\mathrm{d}u}{[(a-u)(b-u)(u-c)(u-d)]^{1/2}} = \pm\frac{1}{\sqrt{2}}(\phi - \phi_0), \quad (c \leq \chi \leq b), \tag{A3}$$

where ϕ_0 is a constant. This equation can be rewritten as:

$$\frac{2}{[(a-c)(b-d)]^{1/2}} F(\delta, m) = \pm\frac{1}{\sqrt{2}}(\phi - \phi_0), \tag{A4a}$$

where

$$\delta = \arcsin\left[\frac{(b-d)(\chi-c)}{(b-c)(\chi-d)}\right]^{1/2}, \quad m = \frac{(b-c)(a-d)}{(a-c)(b-d)}, \tag{A4b}$$

and F, the elliptic integral of the first kind, is defined as

$$F(\delta, m) = \int_0^{\delta} \frac{\mathrm{d}u}{(1 - m\sin^2 u)^{1/2}}. \tag{A4c}$$

Thus, according to the definitions of elliptic functions, we have

$$\frac{(b-d)(\chi-c)}{(b-c)(\chi-d)} = \mathrm{sn}^2[K(\phi-\phi_0), m], \tag{A5a}$$

where

$$K = [(a-c)(b-d)/8]^{1/2}. \tag{A5b}$$

Hence, the periodic solution corresponding to close orbit C can be written as

$$\chi = d + (c-d)\left\{1 - n\mathrm{sn}^2[K(\phi-\phi_0), m]\right\}^{-1}, \tag{A6a}$$

where

$$n = (b-c)/(b-d). \tag{A6b}$$

Note that $0 < n < m < 1$ according to (A4b) and (A6b). From the relation between the coefficients and the roots of the following polynomial:

$$\chi^4 - 2p\chi^2 + 4q\chi + 4C = (a-\chi)(b-\chi)(\chi-c)(\chi-d), \tag{A7}$$

we have

$$a + b + d + c = 0, \tag{A8a}$$

and

$$ab + (a+b)(c+d) + cd = -2p. \tag{A8b}$$

Using (A8a) and introducing the wave weight H measured vertically from trough to crest,

$$H = b - c, \tag{A9}$$

we can express a, b, c and d in terms of m, n and H. These expressions are given here:

$$a = H\,[m(1-2n) + n(2-n)]\,[4n(m-n)]^{-1}, \tag{A10a}$$

$$b = H\,[m(1+2n) - n(2+n)]\,[4n(m-n)]^{-1}, \tag{A10b}$$

$$c = H\,[m(1-2n) - n(2-3n)]\,[4n(m-n)]^{-1}, \tag{A10c}$$

$$d = H\,[-m(3-2n) + n(2-n)]\,[4n(m-n)]^{-1}. \tag{A10d}$$

On substitution of (A10) into (A5b), the expression for K can be rewritten as

$$K = H\sqrt{(1-n)[8n(m-n)]^{-1}}. \tag{A11}$$

The corresponding periodic solution to (3.9), $\zeta = r + \chi$ (see (3.14b)), can be obtained by substituting (A10) into (A6a):

$$\begin{aligned} \zeta &= r - H[m(3-2n) - n(2-n)][4n(m-n)]^{-1} \\ &+ H(1/n-1)\left\{1 - n\mathrm{sn}^2[K(\phi-\phi_0), m]\right\}^{-1}, \quad \phi = \bar{X} + l\bar{Y} - \omega\bar{T}. \end{aligned} \tag{A12}$$

Substituting (A10) and the expression for p (see (3.14b)) into (A8b), we obtain

$$\begin{aligned} \omega = 3r^2 &+ 3l^2 - H^2[m^2(3 - 4n + 4n^2) \\ &- 2mn(2 - n + 2n^2) + n^2(4 - 4n + 3n^2)][4n(m-n)]^{-2}, \end{aligned} \tag{A13}$$

which indeed is the dispersion relation for the periodic wave given by (A12).

(b) When $q = 0$, the phase portrait is symmetric about the ϑ-axis (see figure A2); $\beta = 0$ and $\alpha = -\gamma = p^{1/2}$. When $0 < C < C_\alpha = -f(p^{1/2})$, there exists a close orbit surrounding the origin. In this situation, $f(\chi) + C = 0$ has four distinct real roots, i.e. $\pm a, \pm b$ with $b < a$.

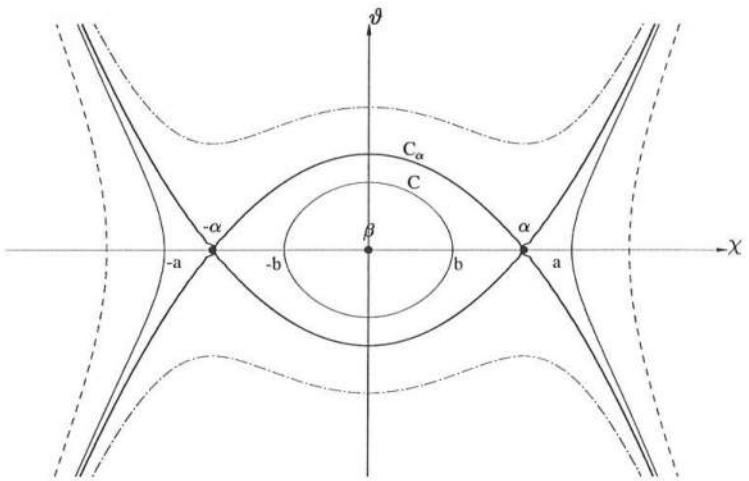

Figure A2: Phase portrait of system (A1) when $p > 0$ and $q = 0$.

Since the orbit is symmetric about the χ- and ϑ-axis, the periodic solution corresponding to close orbit C can be obtained by integrating the first integral (A2) along the orbit in the first quadrant:

$$\int_0^{\chi} \frac{\mathrm{d}u}{[(a^2-u^2)(b^2-u^2)]^{1/2}} = \frac{1}{\sqrt{2}}(\phi - \phi_0), \quad (0 \le \chi \le b). \tag{A14}$$

The integral on the left-hand side again can be recast in terms of the elliptic integral of the first kind F:

$$F(\arcsin(\chi/b), b/a) = \frac{a}{\sqrt{2}}(\phi - \phi_0), \tag{A15}$$

which can be rewritten as:

$$\chi = b\mathrm{sn}\left[\frac{a}{\sqrt{2}}(\phi - \phi_0), b/a\right]. \tag{A16}$$

For convenience, the constants a and b are expressed in terms of the wave height H and the modulus m $(0 < m < 1)$ of the snoidal function:

$$b = H/2, \qquad a = b/m = H/(2m). \tag{A17}$$

The corresponding snoidal-wave solution to (3.9) becomes

$$\zeta = r + \chi = r + \tfrac{1}{2} H \mathrm{sn}\left[H/(2\sqrt{2}\,m)(\phi - \phi_0)\right], \quad \phi = \bar{X} + l\bar{Y} - \omega\bar{T}. \tag{A18}$$

From the relation between the coefficients and the roots of the following polynomial:

$$\chi^4 - 2p\chi^2 + 4C = (a^2 - \chi^2)(b^2 - \chi^2), \tag{A19}$$

we have the following dispersion relation for the snoidal wave (A18):

$$\omega = 3r^2 + 3l^2 - (a^2 + b^2)/2 = 3r^2 + 3l^2 - \tfrac{1}{8} H^2 (1/m^2 + 1). \tag{A20}$$

References

ABLOWITZ, M.J. & CLARKSON, P.A. 1991 *Solitons, Nonlinear Evolution Equations and Inverse Scattering.* Cambridge University Press.

ALPERS, W. & SALUSTI, E. 1983 Scylla and Charybdis observed from space. *J. Geophys. Res.* **88**, 1800–1808.

CHEN, Y. 1995 Modelling of Surface Water Wave and Interfacial Wave Propagation. Doctoral dissertation, Cornell University, Ithaca, New York.

CHEN, Y. & LIU, P. L.-F. 1995 The unified Kadomtsev–Petviashvili equation for interfacial waves. *J. Fluid Mech.* **288**, 383–408.

CHEN, Y. & LIU, P. L.-F. 1996*a* On interfacial waves over random topography. *Wave Motion* **24**, 169–184.

CHEN, Y. & LIU, P. L.-F. 1996*b* Numerical study of surface wave and Kelvin solitary wave propagation in a wide channel. *Fluid Dynamics Research* (in press).

FARMER, D.M. 1978 Observations of long nonlinear internal waves in a lake. *J. Phys. Oceanogr.* **8**, 63–73.

GARGETT, A.E. 1976 Generation of internal waves in the Strait of Georgia, British Columbia. *Deep-Sea Res.* **23**, 17–32.

GRIMSHAW, R. & TANG, S. 1990 The rotation-modified Kadomtsev–Petviashvili equation: An analytical and numerical study. *Stud. Appl. Math.* **83**, 223–248.

HELFRICH, K.R., MELVILLE, W.K. & MILES, J.M. 1984 On interfacial solitary waves over slowly varying topography. *J. Fluid Mech.* **149**, 305–317.

HUNKINS, K. & FLIEGEL, M. 1973 Internal undular surges in Seneca Lake: A natural occurrence of solitons. *J. Geophys. Res.* **78**, 539-548.

KADOMTSEV, B.B. & V.I. PETVIASHVILI, V.I. 1970 On the stability of solitary waves in weakly dispersing media. *Sov. Phys. Dokl.* **15**, 539–541.

KATSIS, C. & AKYLAS, T.R. 1987 Solitary internal waves in a rotating channel: A numerical study. *Phys. Fluids* **30**, 297–301.

LA VIOLETTE, P.E. & ARNONE, R.A. 1988 A tide-generated internal waveform in the western approaches to the Strait of Gibraltar. *J. Geophys. Res.* **93**, 15653–15667.

MAXWORTHY, T. 1983 Experiment on solitary internal Kelvin waves. *J. Fluid Mech.* **129**, 365–383.

MELVILLE, W.K. & HELFRICH, K.R. 1987 Transcritical two-layer flow over topography *J. Fluid Mech.* **178**, 31–52.

MELVILLE, W.K., TOMASSON, G.G. & RENOUARD, D.P. 1989 On the stability of Kelvin waves. *J. Fluid Mech.* **206**, 1–23.

TOMASSON, G.G. & MELVILLE, W.K. 1991 Flow past a constriction in a channel: a modal description. *J. Fluid Mech.* **232**, 21–45.

RENOUARD, D.P., CHABERT D'HIÉRES, G. & ZHANG, X. 1987 An experimental study of strongly nonlinear waves in a rotating system. *J. Fluid Mech.* **177**, 381–394.

THORPE, S.A., HALL, A. & CROFTS, I. 1972 The internal surge in Loch Ness. *Nature* **237**, 96–98.

TSUJI, H. & OIKAWA, M. 1993 Two-dimensional interaction of internal solitary waves in a two-layer fluid. *J. Phys. Soc. Japan* **62**, 3881–3892.

Dr. Yongze Chen, Center for Coastal Studies, Scripps Institution of Oceanography, 9500 Gilman Dr., La Jolla, CA 92093-0209. (fax: 619-534-0300; e-mail: yongze@coast.ucsd.edu)

Received _____